

CARRIER SUITABILITY OF LAND-BASED AIRCRAFT

José-Luis Hernando and Rodrigo Martínez-Val
Universidad Politécnica de Madrid

joseluis.hernando@upm.es;rodrigo.martinezval@upm.es

Keywords: *carrier suitability, naval aviation, airplane performance, aircraft carrier*

Abstract

The paper describes the first steps of a study aimed at assessing the modifications that should be introduced in ground-based combat airplanes to make them compatible with aircraft carriers designed with ski-jumps and arresting devices. The present analysis includes operational and performance aspects, and describes the complexity of the take-off and approach/landing manoeuvres, identifying the key variables intervening in such manoeuvres. A last section is devoted to summarise the most critical features for carrier suitability.

1 General Introduction

Although naval aviation is 100 years old and has experienced an astonishing development [1-3] it is still one of the most challenging environments for airplane operations: extremely small, moving runways; encounters with turbulence from the vessel's superstructure wake or from the rough sea surface; etc. Safe and effective carrier-airplane compatibility is difficult to achieve, and that is why any analysis on naval aviation requires an in-depth understanding of all factors and problems to be taken into account.

Airplanes operating from aircraft carriers perform in two different ways: conventional airplanes that roll on the deck for take-off and landing, although commonly helped by launching and arresting equipment; and vertical/short take-off and landing (V/STOL) aircraft, capable of using its thrust vectoring control (TVC) to become airborne and be recovered vertically or after a very short landing run [4, 5]. In spite of its vertical manoeuvre

capability, these last airplanes usually perform short take-offs and vertical landings, to save fuel and for payload optimization [6]. It is, then, possible to establish a first differentiation of carriers between conventional and V/STOVL ones. The term conventional used here should not be confused with non-nuclear propulsion, because it refers to the type of airplanes operating and not to the ship's power plant. For take-off, conventional airplanes are either assisted by means of a steam catapult (an electromagnetic device will be ready in the coming years) or roll on a deck with an upward-bent (ski-jump) at the end of the deck, to facilitate the take-off manoeuvre [7-9]. Depending on the equipment used to assist the aircraft in the take-off and recovery (landing) manoeuvres the carriers are classified into various categories, as shown in Fig. 1: carriers designed to operate only with TVC airplanes; angled-deck vessels with arresting recovery (STOBAR); and ships equipped with catapults and arresting devices for take-off and recovery, respectively (CATOBAR). Two additional categories, both with continuous decks and arresting devices, with or without catapult for take-off, are not in service anymore. The CATOBAR category requires vessels of enormous size. As a matter of fact the US Navy currently restricts the term "carrier vessel" for the CATOBAR ships. All other, smaller carriers are considered assault ships.

Main ships and fighter airplanes in service are shown in Fig. 1:

- CATOBAR (nuclear propulsion): US CVN's, 95000 tons (F/A-18C, F/A-18E/F, EA-18G); French Charles de

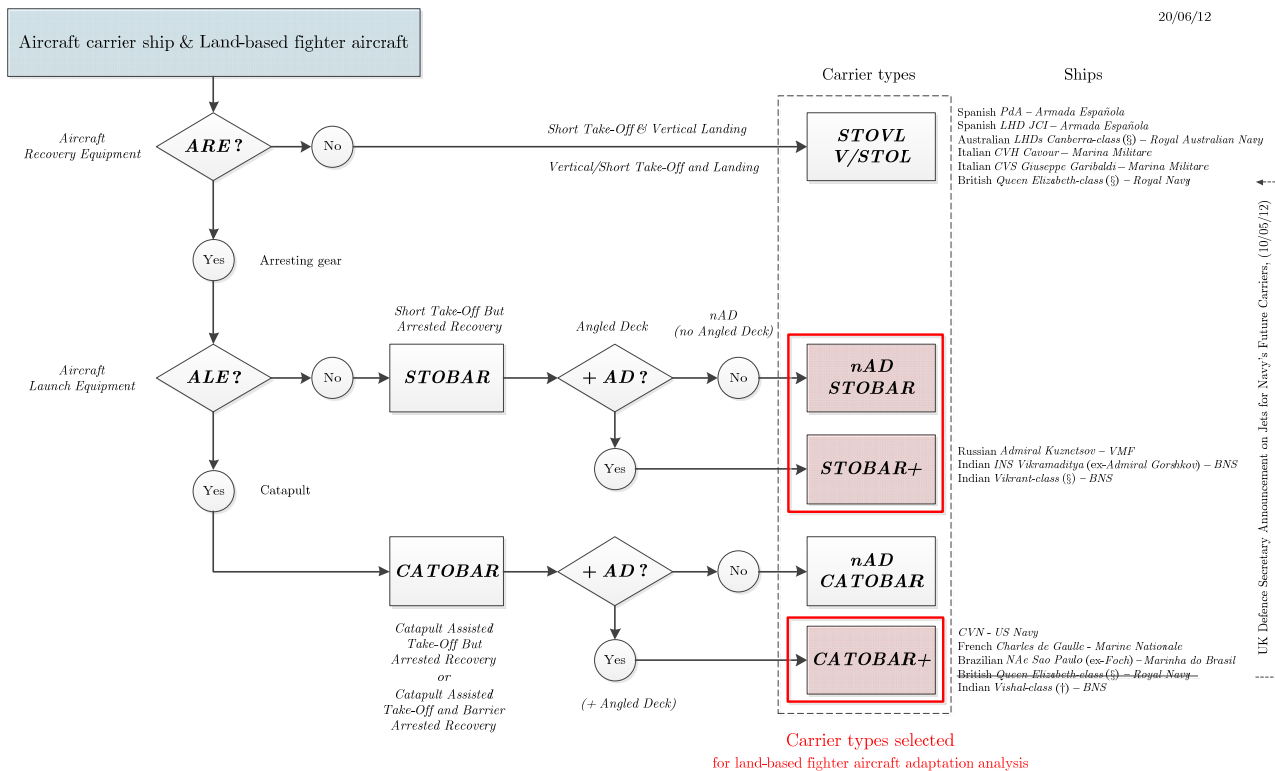


Fig. 1: Carrier types classification scheme.

Symbol notes: (§), under construction; (†), project.

Special acronyms: VMF, *Voyenno-Morskoy Flot Rossii* (Russian Navy). BNS, *Bharatiya Nau Sena* (Indian Navy).

Gaulle, 40000 t (Rafale M, Super-Étendard).

- CATOBAR: Brazilian Sao Paulo (ex-Foch, former French flagship), 30000 t (A-4KU).
- STOBAR: Russian Admiral Kuznetsov, 60000 t (Sukhoi Su-33).

Some other major vessels, in the STOBAR category, are undergoing trials and are expected to be operational rather: the Hindu Vikramaditya (a Russian Kiev-class modification), 45000 t (Mig-29K) and an unknown name Chinese ship (ex-Varyag, originally a twin Kuznetsov), (with J-15, the Chinese adaptation of Sukhoi Su-33). Further, the British Queen Elizabeth-class new design seems to be modified from STOBAR to CATOBAR, according to the British Government Strategic Defence Security Review, to host JSF naval versions around 2015 [10, 11].

Figure 1 also shows a number of carriers specifically designed to operate with V/STOL

airplanes; essentially the BAe AV-8 Harrier and its derivatives [12]. This is the case of some large vessels belonging to the US and Royal Navies, as well as other mid-size carriers sailing with Italian, Spanish, or Indian Navies. New flagship carriers have recently entered into service (the Italian Comte di Cavour and the Spanish Juan Carlos I, both operating Harrier II) or will do soon (Australians Canberra and Adelaide). This naval aviation scenario will change soon, because the British Government has announced in 2010 the withdrawal of its Harriers, and this occurs in parallel to the US plans of mid-term retirement of its 120 V/STOL aircraft. Both decisions will force the navies operating this aircraft type to find suitable replacements, compatible with the existing or planned carriers; since the joint strike fighter program, JSF, is facing increasing costs and delays and will not be available for allied navies within the next decades.

Other alternatives must be studied to keep the operational capabilities of the modern mid-size carriers. The crucial decision is to develop a completely new combat airplane or to adapt an

existing, ground-based design. Potential candidates for this last case, with adequate combat capabilities, would be for example the Eurofighter Typhoon and the Swedish SAAB Gripen.

The present paper describes the first steps of a study (constituting the Doctor Thesis of the first author) to analyse the modifications, essential or convenient, to be introduced in ground-based combat airplane to make them compatible with most STOBAR vessels. Such analysis starts by a description of the take-off manoeuvre performed on a deck with ski-jump at the end, including wind effects and semi ballistic path after lift-off. The next chapter will be devoted to the airplane approach and recovery, performed with the help of arresting equipment. The final considerations will summarise the main findings and will list the next steps in the aircraft navalisation study.

2 Airplane take-off performance from ski-jump carrier

Let us describe the take-off manoeuvre from the deck of an aircraft carrier. The manoeuvre will be performed at zero-wind and the vessel will remain completely static and horizontal. The deck is built with an upward bent at the end, commonly known as ski-jump. To better understand the airplane performance, the take-off is divided into two phases: an ordinary acceleration run over the flat deck and a forced, curved portion until the airplane lift-off from the vessel.

2.1 Take-off run on the flat deck

The common Flight Mechanics equations for the ground run, referred to the centre of mass, and expressed in wind-axes are [13, 14]

$$T \cos(\theta_0 + \varepsilon) - (D + F_R) = \frac{W}{g} \frac{dv}{dt} \quad (1)$$

$$L + T \sin(\theta_0 + \varepsilon) + N - W = 0$$

where W is the aircraft weight, T is thrust, F_R stands for the rolling friction, N is the deck normal reaction, and $\{L, D\}$ are lift and drag

aerodynamic forces, respectively. On another side, θ_0 is the pitch angle between the fuselage reference line and the deck and ε is the thrust set angle, referred again to the fuselage longitudinal-axis.

Integrating the first equation of (1) yields:

$$\int T \cos(\theta_0 + \varepsilon) ds - \int (D + F_R) ds = \frac{W}{g} \int_0^{v_I} v dv \quad (2)$$

Assuming no thrust vectoring control (TVC), small angles and almost constant thrust along the deck run, a mean effective thrust can be defined as:

$$\bar{T} \equiv \frac{1}{L_{Deck}} \int_0^{L_{Deck}} T(s) \cos(\theta_0 + \varepsilon) ds \quad (3)$$

where L_{deck} is the available length for this take-off phase.

Equation 2 can, then, be rewritten to link the aerodynamic and propulsive characteristics to the kinetic energy at the end of the flat run, with speed v_I :

$$\bar{T} L_{Deck} - \int (D + F_R) ds = \frac{1}{2} \frac{W}{g} v_I^2 \quad (4)$$

For common combat naval airplanes the second term of Eq. 4 is very small, as compared to the other terms. Reference [15] estimates it as 2% of the final kinetic energy, for the case of catapult launching, and this is the value adopted also here. Therefore Eq. 4 becomes:

$$\bar{T} L_{Deck} \simeq 1.02 \times \frac{1}{2} \frac{W}{g} v_I^2 \quad (5)$$

To obtain the maximum thrust and thence, the maximum speed at the end of this phase, the airplane will be retained by means of brakes or holdback fittings, with the throttle forward at MIL thrust or afterburner positions.

The achieved end speed will be:

$$v_I = \sqrt{\frac{2}{1.02} g \frac{\bar{T}}{W} L_{Deck}} \quad (6)$$

2.2 Ski-jump manoeuvre

When the airplane enters into the curved, last deck portion, the equations are:

$$T \cos(\theta_0 + \varepsilon) - (D + F_R) - W \sin \theta_{Deck} = \frac{W}{g} \frac{dv}{dt} \quad (7)$$

$$(L + N) + T \sin(\theta_0 + \varepsilon) - W \cos \theta_{Deck} = \frac{W}{g} \frac{v^2}{R}$$

where $R(s)$ is the local radius of curvature and $\theta_{Deck}(s)$ the local tangential deck angle above the horizon.

Again, for this take-off phase we can define a mean effective thrust, \bar{T}_{SJ} for thrust (note that the intervening angles are the same as in the flat deck run), and a mean radius of curvature \bar{R} .

$$\bar{T}_{SJ} \equiv \frac{1}{s_{SJ}} \int_0^{s_{SJ}} T(s) \cos(\theta_0 + \varepsilon) ds \quad (8)$$

$$\bar{R} \equiv \frac{1}{(1 - \cos \theta_f)} \int_0^{s_{SJ}} \sin \theta_{Deck} ds \quad (9)$$

If the ski-jump is shaped as a circular arc, then

$$s_{SJ} = R\theta_f \quad (10)$$

Taking into account Eqs. 8 and 9 and the small influence of the aerodynamic drag and rolling friction [15] it is possible to provide a quadrature for the longitudinal forces of Eq. 7:

$$s_{SJ} \bar{T}_{SJ} - W \bar{R} (1 - \cos \theta_f) = 1.02 \times \frac{1}{2} \frac{W}{g} (v_{II}^2 - v_I^2) \quad (11)$$

which results in:

$$v_{II} = \sqrt{v_I^2 + \frac{2}{1.02} g \left[s_{SJ} \frac{\bar{T}_{SJ}}{W} - \bar{R} (1 - \cos \theta_f) \right]} \quad (12)$$

2.3 Wind-on-deck effects

In naval operations it is always necessary to consider the effect of wind, either natural or (more commonly) due to ship propulsion. Wind appears as a constant, aligned wind-on-deck speed v_{OD} (no cross-wind is considered).

2.3.1 Flat deck run

The wind-on-deck speed will result in an increase of any aerodynamic force, F , as:

$$\left(\frac{\Delta F}{F} \right)_{v_{OD}}^I = \frac{(v_I + v_{OD})^2 - v_I^2}{v_I^2} = 2 \frac{v_{OD}}{v_I} + \left(\frac{v_{OD}}{v_I} \right)^2 \quad (13)$$

The lift increase will reduce the normal and frictional forces, but we can assume that this will be compensated by the drag increment.

2.3.2 Curved deck run

In the ski-jump, the wind increases the speed and the angle of attack, as shown in Fig. 2. The increase in angle of attack is:

$$\Delta \alpha = \arctan \left(\frac{v_{OD} \sin \theta}{v + v_{OD} \cos \theta} \right) \simeq \frac{\sin \theta}{1 + \frac{v_{OD}}{v} \cos \theta} \quad (14)$$

Consequently, the aerodynamic lift rises up to:

$$L_{v_{OD}}^{II} = \frac{1}{2} \rho_0 \left[(v \cos \theta + v_{OD})^2 + (v \sin \theta)^2 \right] S C_L (\alpha + \alpha_0 + \Delta \alpha) \quad (15)$$

And the lift increment will be:

$$\left(\frac{\Delta L}{L} \right)_{v_{OD}}^{II} = \frac{\Delta \alpha}{(\alpha + \alpha_0)} + \left[2 \frac{v_{OD}}{v} \cos \theta + \left(\frac{v_{OD}}{v} \right)^2 \right] \left[1 + \frac{\Delta \alpha}{(\alpha + \alpha_0)} \right] \quad (16)$$

At the end of the ski-jump, corresponding to $\theta = \theta_f$ and $v = v_{II}$:

$$(\Delta \alpha)_{v_{II}} \simeq \frac{\sin \theta_f}{1 + \frac{v_{OD}}{v_{II}} \cos \theta_f} \quad (17)$$

$$\left(\frac{\Delta L}{L} \right)_{v_{OD}}^{II} = \frac{(\Delta \alpha)_{v_{II}}}{(\alpha + \alpha_0)} + \left[2 \frac{v_{OD}}{v_{II}} \cos \theta_f + \left(\frac{v_{OD}}{v_{II}} \right)^2 \right] \left[1 + \frac{(\Delta \alpha)_{v_{II}}}{(\alpha + \alpha_0)} \right]$$

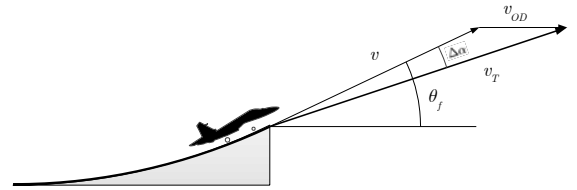


Fig. 2: Wind-on-deck effect in the ski-jump: increase in speed and angle of attack.

2.4 Some take-off examples

Let us now consider two representative ships: the Spanish Juan Carlos I and the Russian Admiral Kuznetsov (see Fig. 3). These ships have been selected because of their configuration and because they have been designed to host two different airplane concepts: the STOVL Harrier for Juan Carlos I, and the

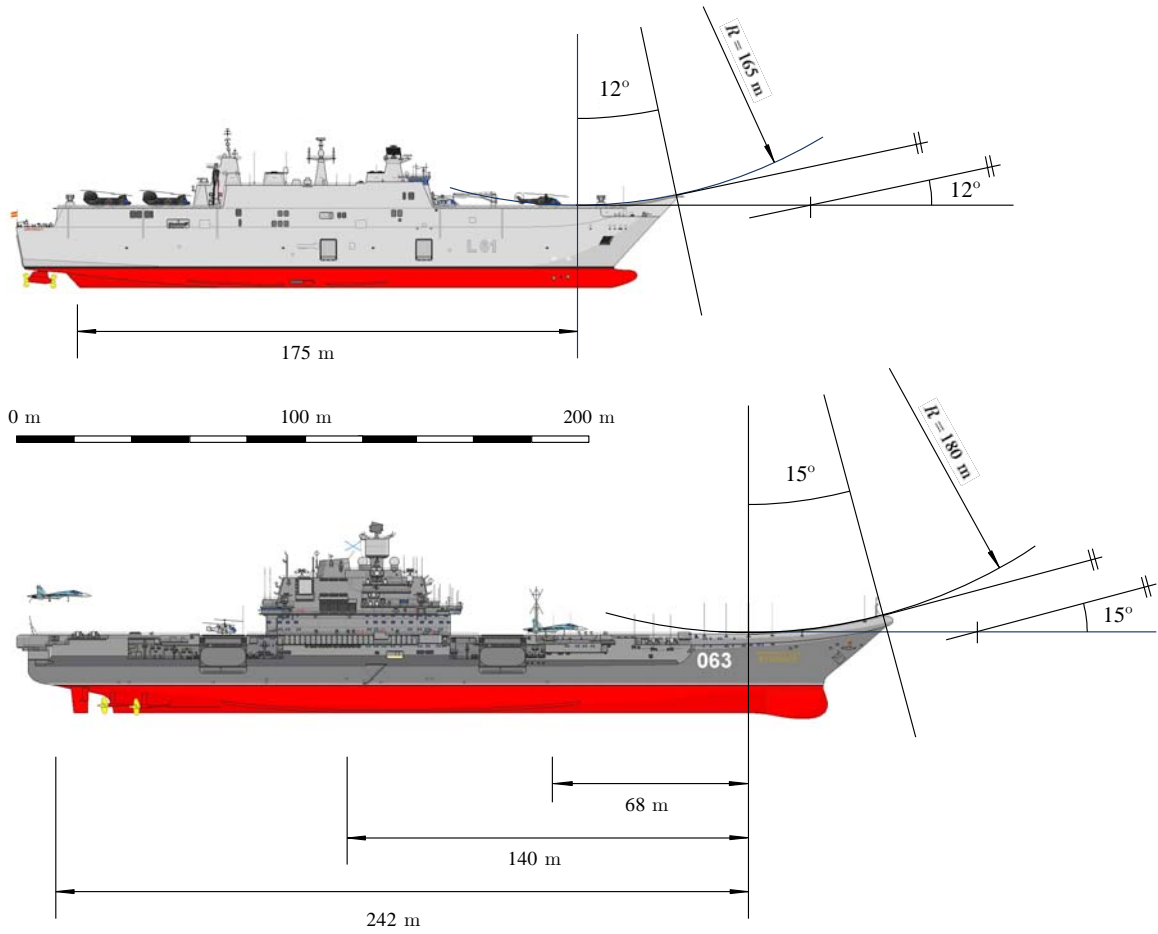


Fig. 3: Side view and dimensions of the Spanish Juan Carlos I (JCI), top, and Russian Admiral Kuznetsov, bottom, from Ref. [16].

conventional Su-33 for the Kuznetsov. Since the Harrier will soon be out of operation, the aircraft-vessel compatibility will be done here with the Eurofighter Typhoon hypothetically operating from the Juan Carlos I.

To simplify the present analysis, the ski-jump shape of both vessels is approximated by a circular arc, and the angle of attack¹ of the airplane and the wind-on-deck are assumed to be:

$$\alpha + \alpha_0 = 12^\circ ; \quad v_{OD} = 20 \text{ knot} \quad (18)$$

Equation 10 becomes:

$$s_{SJ} = \bar{R}\theta_f \quad (19)$$

¹ To obtain such angle of attack it might be necessary to set the wing incidence at root, increase the nose landing gear (NLG) length, etc.

2.4.1 Su-33 operation from Admiral Kuznetsov

The main data to be used for this airplane-vessel couple are $T/W=0.89$ (see Fig. 4) and $\bar{R} = 180 \text{ m}$; $\theta_f = 15^\circ$; $L_{Deck} = 140 \text{ m}$ (20)

which results in

$$(v_I)_{Kuzn,140m}^{Su-33} = 48.9 \text{ m/s}$$

$$(v_{II})_{Kuzn,140m}^{Su-33} = 55.5 \text{ m/s}$$

$$\left(\frac{\Delta F}{F}\right)_{v_{OD}}^I \Big|_{Kuzn,140m}^{Su-33} = 46\% \quad (21)$$

$$\left(\Delta\alpha\right)_{v_{II}} \Big|_{Kuzn,140m}^{Su-33} = 2.3^\circ$$

$$\left(\frac{\Delta L}{L}\right)_{v_{OD}}^{II} \Big|_{Kuzn,140m}^{Su-33} = 66.3\%$$

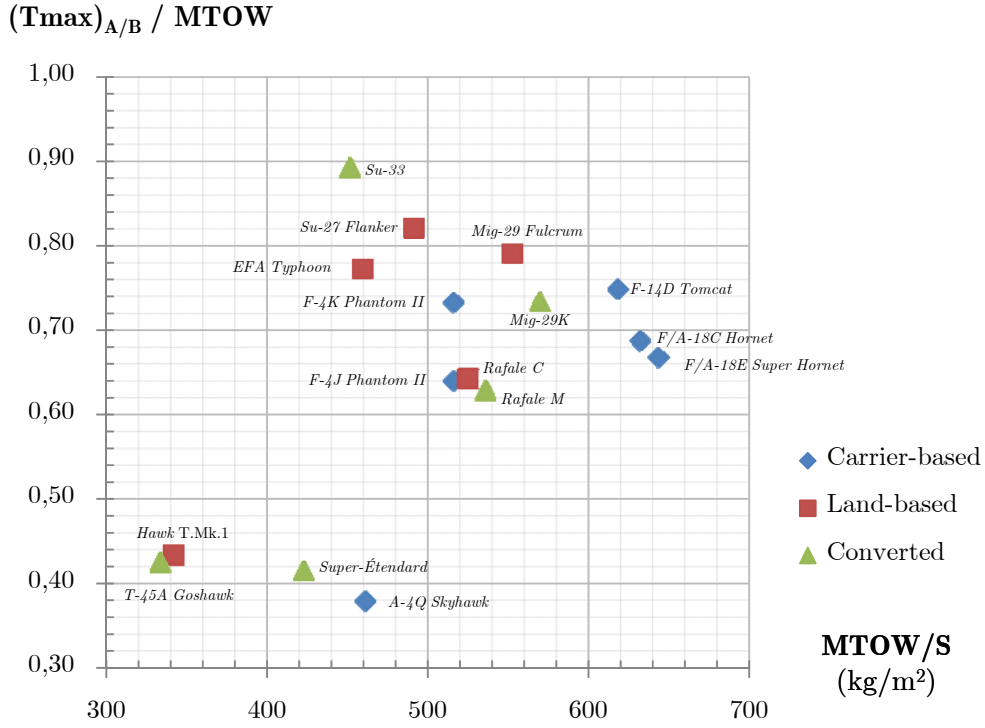


Fig. 4: Thrust-to-weight ratio (with afterburner) and maximum wing loading for some airplanes of interest (carrier-based, land-based and converted). Data from Ref. [17].

2.4.2 EFA operation from Juan Carlos I

In this case $T / W = 0.77$ (see Fig. 4) and $\bar{R} = 165 \text{ m}$; $\theta_f = 12^\circ$; $L_{Deck} = 175 \text{ m}$ (22)

which leads to

$$\begin{aligned}
 (v_I)_{JCI,175m}^{EFA} &= 50.9 \text{ m/s} \\
 (v_{II})_{JCI,175m}^{EFA} &= 55.1 \text{ m/s} \\
 (\Delta F / F)_{v_{OD}}^I \Big|_{JCI,175m}^{EFA} &= 44.5\% \quad (23) \\
 (\Delta \alpha)_{v_{II}} \Big|_{JCI,175m}^{EFA} &= 1.9^\circ \\
 (\Delta L / L)_{v_{OD}}^{II} \Big|_{JCI,175m}^{EFA} &= 62\%
 \end{aligned}$$

2.5 Semi-ballistic flight and launching compatibility

When an airplane takes-off from a curved-deck it suddenly jumps into free air. The objective is to approximately reach the suitable speed and angle of attack, at the end of the ski-jump, without exactly respecting the airplane lift to weight equilibrium: it may well be in an infra-lift² condition. The strategy aims at keeping the longitudinal acceleration by maintaining engine thrust, and giving full control to the pilot who, until this moment has hardly intervened in the manoeuvre. An acceptable airplane-vessel compatibility matching implies that the flight speed will reach a minimum value to sustain level flight before the airplane altitude over the sea crosses below a certain safety threshold.

To accomplish that matching, all variables in the above equations and requirements must satisfy a set of coupled relationships

$$\{W, T, L_{Deck}, (\theta_0 + \varepsilon), \bar{R}, \theta_f, C_L, C_D, S, v_{OD}\} \quad (24)$$

² Infra-lift means that lift is not sufficient to equilibrate vertically the airplane, so it would fall with increasing speed after a brief soaring (semi-ballistic flight).

to provide $v_I, v_{II}, (\Delta\alpha)_{v_{II}}, (\Delta F)_{v_{OD}}, (\Delta L)_{v_{OD}}$ and solve the three degrees of freedom (vertical, horizontal and pitching) from known initial conditions

$$v(0) = v_{II}; \quad \gamma(0) = \theta_f; \quad \dot{\theta}(0) = v_{II} / \bar{R}; \quad \theta(0) = \theta_f \quad (25)$$

The overall result must meet all safety and performance criteria at an airplane take-off weight acceptable in terms of mission effectiveness. Any other solution has to be discarded.

3 Aircraft recovery and arresting

When an airplane is approaching the deck of a vessel, following certain glide path γ , at constant speed v (see Fig. 5) the equations are

$$\begin{aligned} L \cos \gamma + D \sin \gamma + T \sin(\varepsilon + \theta) &= W \\ T \cos(\varepsilon + \theta) + L \sin \gamma &= D \cos \gamma \end{aligned} \quad (26)$$

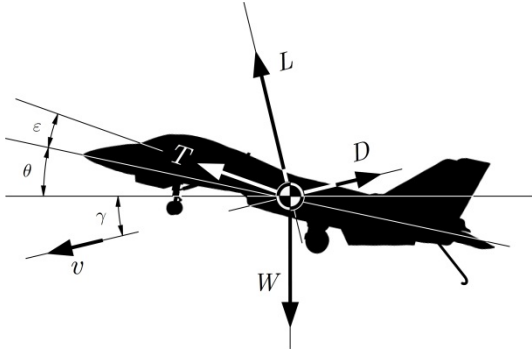


Fig. 5: Airplane forces and attitude in descending flight.

Assuming all angles are small

$$\gamma \sim (\varepsilon + \theta) \ll 1 \quad (27)$$

and a difference in force order of magnitude

$$L \sim T \sim W \gg D \quad (28)$$

the vertical equilibrium of Eq. 26 can be expressed as

$$W \simeq L = \frac{1}{2} \rho_0 (v_{ref})^2 S (C_L)_{ref} \quad (29)$$

where the subscript *ref* (for reference) stands for diverse cases to be considered: wave-off, pop-up manoeuvre, etc; to determine the most appropriate one. It must be noticed that naval operations require a *powered approach*, for the

case when the airplane does not engage the arresting equipment and has to accelerate and lift off again [18, 19].

3.1 Approach strategies and conditions

Carrier operations must take into account atmospheric conditions, specifically wind, vessel motion and vessel topology, particularly aligned or angled decks.

3.1.1 Carrier landing pattern

Figure 6 shows the complexity of such operations in the most common case of an angled deck, when the airplane flies a hippodrome circuit (carrier landing pattern, CLP, [20]) around the vessel. Besides boltering and wave-offs, there are additional considerations about visibility, emergency situations, formation approaches, etc.

3.1.2 Wind-on-deck at angled deck carriers

It is possible to compose the ship motion with the atmospheric wind to obtain a certain wind-on-deck orientation. The component of this wind parallel to the landing area centerline is called recovery headwind (RHW). So, with an adequate heading χ the approaching airplane can find zero cross-wind to maximize RHW and improve recovery conditions (see Fig. 7).

$$\sin \chi = \frac{v_{OD}}{v_{wind}} \sin \psi \quad (30)$$

In this way the airplane seems to fly pursuing the ramp. That is why this scheme is called *ramp pursuit* approach.

This configuration may assist in minimizing burble; i.e. the intersection of the superstructure wake with the airplane path [21].

In the other hand, if the ship sails heading the atmospheric wind, the resulting wind-on-deck will sweep the deck along the longitudinal axis of the ship from bow to stern. In this case, the airplane has to choose between two flying techniques: i.e. with or without sideslip (without

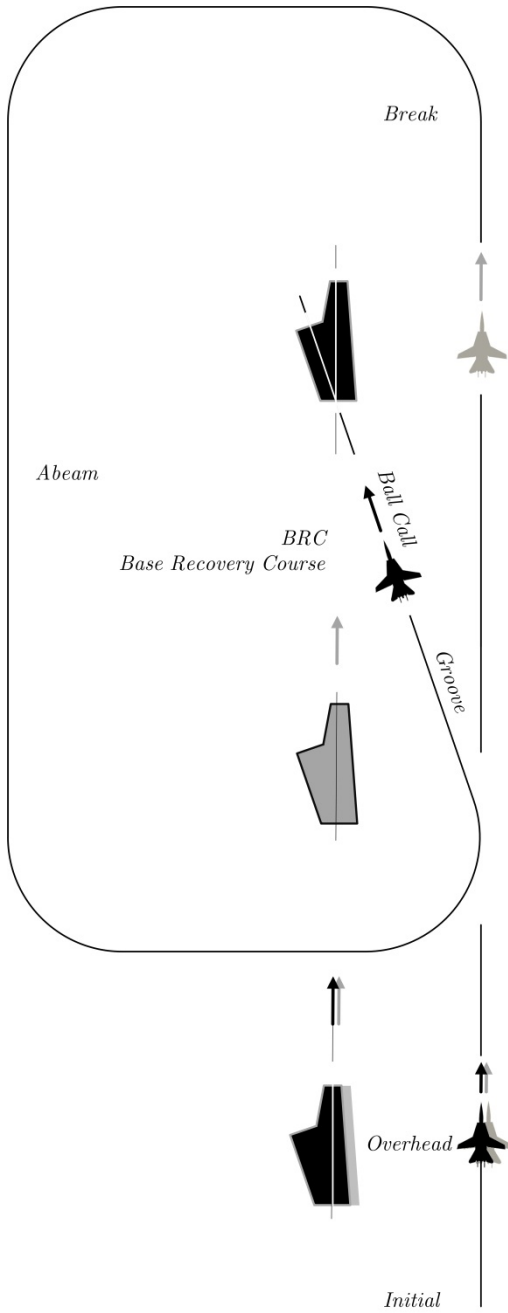


Fig. 6: US Navy's simplified Carrier Landing Pattern (CLP), Case I.

sideslip, for an observer on the deck the airplane seems to fly pursuing the bow, thus is called *bow pursuit*). Figure 8 presents both situations. When flying with sideslip, the airplane is banked, that implies no level wings, a major disadvantage in naval operations.

The apparent sideslip angle β_1 (azimuthal) is:

$$\beta_1 = \arcsin \left(\frac{v_{OD} \sin \psi}{v_{ref} \cos \gamma} \right) \quad (31)$$

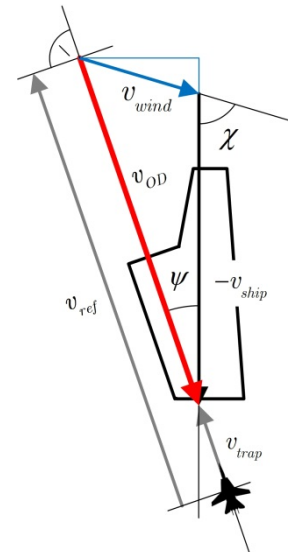


Fig. 7: Ramp pursuit scheme.

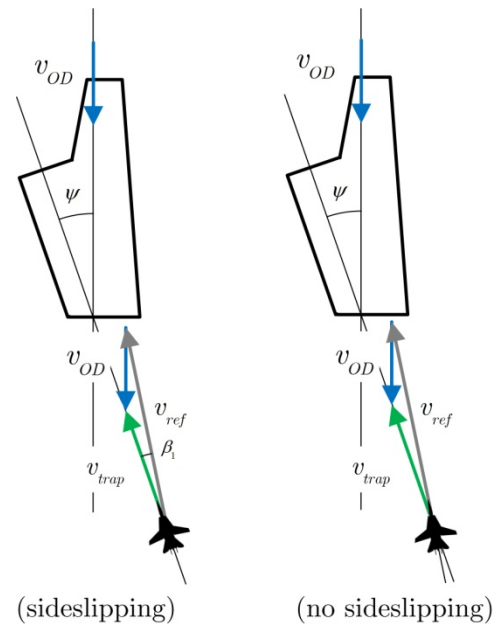


Fig. 8: Bow pursuit (right) explanation drawing.

Ref. [20] prefers ramp pursuit configuration, though this obliges the ship to maintain proper heading and speed according to Fig. 7, but not correcting it while an airplane is approaching.

3.2 Touchdown and braking

Let us now consider that the ship is heading against the atmospheric wind and the airplane approaches without sideslip (wings levelled).

The composed wing forms an angle ψ with respect to the ship longitudinal axis. The geometry describing this approach is depicted in Figs. 9 and 10, differentiating flight path γ and optical glide slope ϕ . New trap and engaging velocities are defined; the names alluding to the use of arresting gear:

- Trap speed v_{trap} is the flight speed relative to the angled deck;
- Engaging speed $v_{engaging}$ is the deck projection of the trap speed; i.e. the speed directly involved in the arresting physics.

$$\vec{v}_{trap} = \vec{v}_{ref} - \vec{v}_{OD}$$

$$v_{sink} = v_{ref} \sin \gamma \quad (32)$$

$$v_{engaging} = v_{ref} \cos \gamma - v_{OD} \cos \psi$$

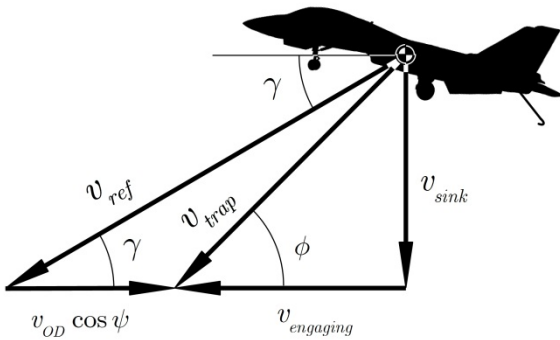


Fig. 9: Kinematics of an airplane descending to a moving angled deck

The quotient between these two speeds is

$$\cos \phi = \frac{v_{engaging}}{v_{trap}} \quad (33)$$

This angle ϕ is the glide slope angle relative to the deck and it is used by IFLOLS, an optical approach aid using Fresnel Lenses. This system is a primary reference in the final approach to the ship (from 0.6 nm to ramp) [22, 23].

Angles ϕ, γ are related as

$$\frac{1}{\cos \phi} = \frac{1}{\left(\cos \gamma - \frac{v_{OD}}{v_{ref}} \cos \psi \right)} \sqrt{\sin^2 \gamma + \left(\cos \gamma - \frac{v_{OD}}{v_{ref}} \cos \psi \right)^2} \quad (34)$$

Concerning the kinetic energy of the airplane

$$\left(E_{Kinetic} \right)_{WOD} = \frac{1}{2} \frac{W}{g} \left(v_{sink}^2 + v_{engaging}^2 \right) \quad (35)$$

it has to be unevenly absorbed by the airplane landing gear and the arresting gear:

$$E_{Kinetic, LG} = \frac{1}{2} \frac{W}{g} v_{sink}^2 \quad (36)$$

$$\left(E_{Kinetic, AG} \right)_{WOD} = \frac{1}{2} \frac{W}{g} v_{engaging}^2$$

It is easy to appreciate that the wind-on-deck decreases the energy to be absorbed by the arresting gear:

$$\left(\Delta E_{Kinetic, AG} \right)_{WOD} = \left(1 - \frac{v_{OD} \cos \psi}{v_{ref} \cos \gamma} \right)^2 - 1 \quad (37)$$

However, since the airplane keeps most of its thrust, the total energy to be dissipated is

$$E_{t, WOD} = \frac{1}{2} \frac{W}{g} \left(v_{sink}^2 + v_{engaging}^2 \right) + T \left(\Delta s \right)_{trap} \quad (38)$$

including the work done by the engine thrust during the arresting run (the effect of drag and friction have been neglected).

Finally, the total energy to be absorbed by the arresting gear mechanism is

$$\left(E_{t, AG} \right)_{WOD} \simeq \left(E_{Kinetic, AG} \right)_{WOD} + T \left(\Delta s \right)_{trap} \quad (39)$$

$$= \frac{1}{2} \frac{W}{g} v_{ref}^2 \left(\cos \gamma - \frac{v_{OD}}{v_{ref}} \cos \psi \right)^2 + T \left(\Delta s \right)_{trap}$$

3.3 Wind-on-deck effect example

Taking some representative values of combat airplanes in naval operations

$$\begin{aligned} W &= 30000 \text{ lb} \\ v_{OD} &= 20 \text{ knot}; \quad \phi = 3.5^\circ \\ v_{ref} &= 160 \text{ knot}; \quad \psi = 9^\circ \end{aligned} \quad (40)$$

Equations 32 to 38 provide

$$\begin{aligned}
 \beta_1 &= 1.22^\circ \\
 v_{engaging} / v_{trap} &= 0.998; \quad \gamma \simeq 3.1^\circ \\
 v_{engaging} &= 140 \text{ knot} \simeq v_{trap}; \\
 (E_{Kinetic,AG})_{WOD} &= 35.3 \text{ MJ} = 9.8 \text{ kW-h} \\
 (\Delta E_{Kinetic,AG})_{WOD} &= -23.2\%
 \end{aligned} \quad (41)$$

3.4 Safe recovery considerations

The ship arresting equipment consists of several traverse arresting cables, pendants, placed along the touching area. The airplane approaches the ship at an attitude depending on its aerodynamic and control features. Figure 10 shows the importance of two key variables: the hook-to-eye, H/E, and hook-to-ramp, H/R, distances to guarantee that the airplane engages at least one of the arresting cables without crashing on the deck leading edge. The IFLOLS information must take into account both H/E and H/R (see Fig. 10).

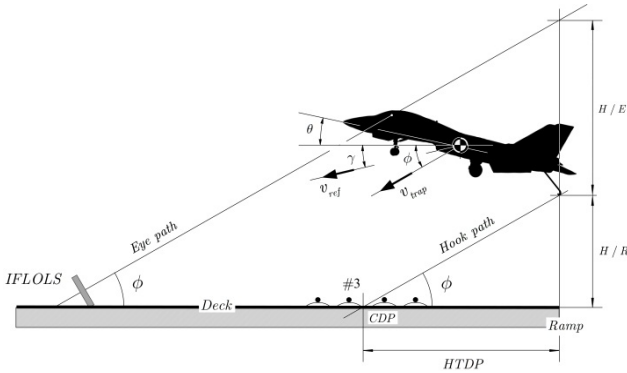


Fig. 10: Airplane approaching to a deck in motion, showing several distances and angles definitions.

All former descriptions correspond to a static ship, except for a horizontal, known, motion. However, actual operations occur in a variety of sea conditions and airplane operations must be safe within the majority of them, which do not correspond to such ideal fully horizontal deck. For example, according to [22], US Navy carriers rarely exceed

$$\delta\theta = \pm 1.5^\circ \quad (42)$$

$$\delta z = 5.5 \text{ ft}$$

in pitch and heave, respectively.

These ship displacements create an uncertainty on where the hook tip (HTDP) will actually touch. Considering that the pilot does not alter

the airplane path despite the change in visual reference (or supposing that the deck moves in the last fraction of a second), according to Fig. 10 and 11 this results in

$$\begin{aligned}
 (\delta s)_{HTDP} &= (\delta s)_{Heave} + (\delta s)_{Pitch} \\
 &= \frac{\delta z}{\tan \phi} + \frac{\tan \delta\theta \sqrt{1 + \cos^2 \psi \tan^2 \delta\theta}}{(\tan \phi + \cos \psi \tan \delta\theta)} d
 \end{aligned} \quad (43)$$

where d is the pitch moment arm distance; i.e. the longitudinal distance from the ship centre of mass to the nominal touchdown point (between #2 and #3 pendants).

Taking $\hat{d} = 137.5 \text{ ft}$ (estimated from [22]), and considering (41) and (42), Equation 44 gives

$$(\delta s)_{HTDP} = 89.9 + 41.4 \simeq \pm 130 \text{ ft} (= \pm 40 \text{ m}) \quad (44)$$

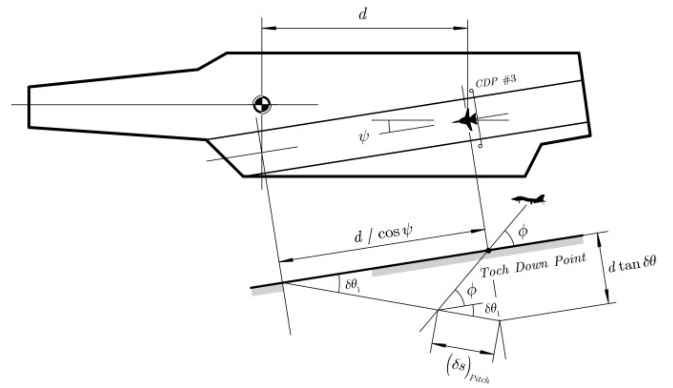


Fig. 11: Effect of deck pitch angle $\delta\theta$ on touchdown point location $(\delta s)_{Pitch}$

H/R distance and $(\delta s)_{HTDP}$ explain why it is necessary to move the touchdown point backwards from the ramp. It is interesting to compare the former result to available distances in actual or programmed carriers shown in Figure 12. In a Nimitz class vessel the distance from the deck edge to #1 pendant is 169 ft 9 in, and the length between #1 and #4 pendants is 121 ft 5 in.

If the airplane does not catch any pendant (or if they break) the airplane will have to accelerate along the remaining deck to become airborne again. The standard procedure is, then, to approach at 80% of full throttle and advance to MIL thrust or A/B throttle as soon as the main landing gear touches on the deck, waiting for the arresting deceleration to bring the throttle back to idle. Thence, Eqs. 39 and 40 include thrust T in the energy dissipation count.

The angled deck allows concurrent operations: typically, a cleared runway for recovery and a front to bow portion for launchings. Figure 12 compares two carrier concepts: a CATOBAR US Navy CVN and the Russian STOBAR (ski-jumped deck for launching) Admiral Kuznetsov.

3.5 Arresting gear features

After the airplane touches on the deck, an ideal run with almost constant deceleration can be considered. In this ideal performance the average arresting load factor is

$$\bar{n}_x = \frac{\bar{a}_x}{g} = \frac{v_{engaging}^2}{2(\Delta s)_{trap}} \quad (45)$$

The ideal landing run length, $(\Delta s)_{trap}$ is the distance between two points : the first one corresponds to the hook tip located at the nominal touchdown point (for example between pendants #2 and #3); and the second one corresponding to the nose landing gear located close to the runway final edge. Some safety margins should be considered.

From Fig. 12

$$(\Delta s)_{trap}|_{CVN} = 155 \text{ m}; \quad (\Delta s)_{trap}|_{Kuznetsov} = 130 \text{ m} \quad (46)$$

Note that both values are about 65% of the maximum landing runway distance. With data shown in (46), Eq. 45 provides

$$(\bar{n}_x)_{NAG,CVN} = 1.7; \quad (\bar{n}_x)_{NAG,Kuznetsov} = 2 \quad (47)$$

These are ideal reference values, because a constant deceleration would imply a constant braking force from touchdown to complete arresting, and thus independent from speed. However, this performance would not be consistent with the requirement of becoming airborne again should the airplane fail from engaging the arresting pendants. It is very important to understand that arresting devices are absolutely necessary to recover airplanes in a short moving deck. Ref. [25] describes the VECTOR programme of experimental landings, using an X-31 airplane. Even with TVC, special flight data sensors and precision GPS to guide the approach, the

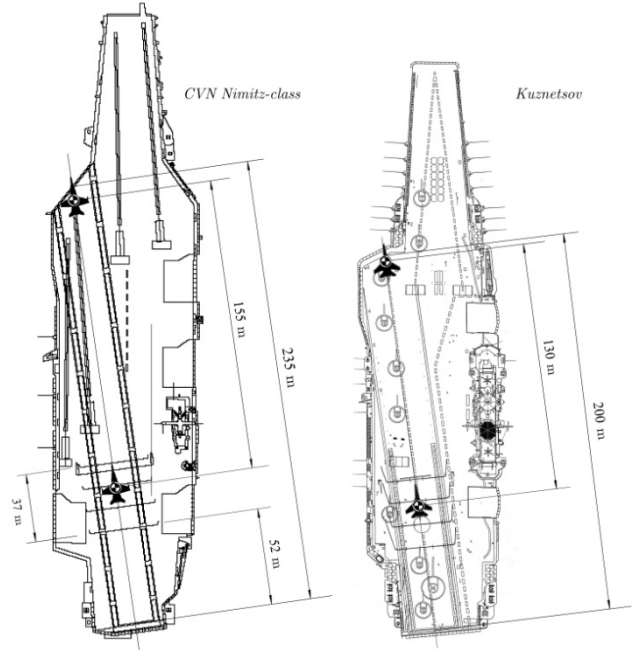


Fig. 12: Plan view of two different carrier types, showing the deck configuration, main operational equipment and major deck distances [24].

automatic flight mode resulted in so high pitch attitude that there was no visibility and a TV camera was needed. Only in the last second, immediately before touchdown, the plane pitched down to avoid damaging its tail. According to (44), this procedure is absolutely incompatible with a moving deck.

This is the meaning of the subscripts -NAG in (47): *No Arresting Gear*.

When the hook engages, the longitudinal equation includes an arresting gear tow force F_{Tow} :

$$T \cos(\theta_0 + \varepsilon) - (F_{Tow} + D + F_R) = \frac{W}{g} v \frac{dv}{ds} \quad (48)$$

that can be integrated to

$$\int_0^{R_{Stroke}} [(F_{Tow} + D + F_R) - T \cos(\theta_0 + \varepsilon)] ds = \frac{1}{2} \frac{W}{g} v_{engaging}^2 \quad (49)$$

where R_{Stroke} is the arresting gear stroke; a system feature. For example, in the US Navy Mk7-3 arresting engine [15]

$$(R_{Stroke})_{MK7-3} = 340 \text{ ft} \quad (50)$$

The arresting engine performance is adjusted to the features of the airplane to be recovered. Reference [15] shows arresting force diagrams, for some thrust-to-weight ratio and engaging speeds:

$$\frac{R_{Stroke}}{W} \frac{1}{g} v_{engaging}^2 \int_0^1 F_{Tow} d(s / R_{Stroke}) \Big|_{T/W=0.4} \simeq 0.55 \quad (51)$$

that provides a statistical maximum tow force, for the appropriate sizing of the arresting hook and airplane structural reinforcements required. For example, for a maximum recovery weight $W_{max} = 40000$ lbf and $v_{engaging} = 140$ knot, Ref. [15] provides

$$(F_{Tow})_{max} = 160 \text{ kips} \quad (52)$$

representing a maximum load factor of

$$(n_x)_{AG,max} = \frac{(F_{Tow})_{max}}{W_{max}} = 4 \quad (53)$$

that can be compared to the results in Eq. 47.

Considering a limit load safety factor $(SF)_y$ and an allowable stress of 80% the yield stress σ_y , it is possible to estimate the arresting hook cross section A_σ as:

$$A_\sigma \geq \frac{(F_{Tow})_{max} \times (SF)_y}{0.8 \times \sigma_y} \quad (54)$$

For *AerMet 100* ultra-high strength martensitic alloy steel

$$\sigma_y = 250 \text{ ksi} (= 1720 \text{ MPa}) \quad (55)$$

From (54):

$$A_\sigma \geq 4 \text{ in}^2 = 2580.64 \text{ mm}^2 \quad (56)$$

For the case of a cylindrical tube with external diameter of

$$(\hat{D}_e)_{Tailhook} = 120 \text{ mm} \quad (57)$$

the minimal wall thickness is

$$\hat{t}_{Tailhook, \hat{D}_e=120 \text{ mm}} \geq 7.3 \text{ mm} \quad (58)$$

3.6 Thrust estimation complying simple bolter requirement

If the hook does not engage any pendant, the airplane has to accelerate as much as possible to become airborne again.

The distance $(\Delta s)_{Bolter}$ can be estimated in a similar way to $(\Delta s)_{trap}$, between the positions corresponding to the hook tip located just behind pendant #4 and the landing deck final

edge. Pilot reaction time and safety margins must be included in any case.

Assuming constant acceleration, and neglecting thrust set angle, drag and friction

$$\frac{1}{2g(\Delta s)_{Bolter}} \left[(v_x)_{f,Bolter}^2 - v_{engaging}^2 \right] = \frac{a_x}{g} \simeq \frac{\hat{T}_{Bolter}}{W} \quad (59)$$

where $(v_x)_{f,Bolter}$ is the minimum speed to

become airborne again, which provides a link between the thrust-to-weight ratio and the available deck length.

4 Final considerations

The present paper has described the take-off and approach/landing manoeuvres, as they are performed on aircraft carriers equipped with ski-jumps and arresting mechanisms. The operations are very different from those on ordinary runways, for the size and longitudinal motion of the deck, for the pitch and heave displacements of the carrier, and for the potential interference between the carrier superstructure wake or the rough sea generated air turbulence and the approach glide path. The findings include the following critical items:

- The thrust-to-weight ratio at take-off must be appropriately matched to the available deck length and the ski-jump geometry, including wind-on-deck effects;
- The approach speed must be compatible with wind-on-deck and the available landing distance to completely stop the airplane after engaging the last arresting pendant;
- The thrust-to-weight ratio at approach must be high enough as to allow fast acceleration and safe lift-off should the airplane hook failing engaging the arresting pendants.

Obviously, since the present paper only describes the first steps of the study there are other important aspects that will be addressed in future works. They include, for example:

- Very fast control to give the pilot full authority on the aircraft after the semi-

ballistic jump at the end of a hands-off take-off;

- Suitable aircraft attitude during ground runs, that may require meaningful modifications of the nose landing gear; and
- Rear fuselage modifications to fit the arresting hook, as well as structural reinforcements to withstand the hook transmitted loads.

References

- [1] Friedman, N., *US aircraft carriers: an illustrated history*. Naval Institute Press, Annapolis, MD, 1983.
- [2] Lawrence, T. *Milestones and developments in US naval carrier aviation*. AIAA 2003-5543. August 2003.
- [3] Lawrence, T. *Milestones and developments in US naval carrier aviation-Part II*. AIAA 2005-6120. August, 2005.
- [4] Izaka, D., *Thrust vectoring nozzle for modern military aircraft*. NATO R&T Organization symposium on active control technology (...). May, 2000.
- [5] Scott, R., *Rolling Recovery. Shipborne Rolling Vertical Landing*. Jane's Defence Weekly, April 2009
- [6] Taylor, D., *The operation of fixed-wing V/STOL aircraft from confined spaces*. Thesis, University of Southampton, 1974.
- [7] Furey, Roger J., *Short takeoff performance using gravity assist ski jump*. David W. Taylor Naval Ship Research and Development Center. WRDC-TM-90-337-FIBE, 1983.
- [8] WRDC-TM-90-337-FIBE. Turner, E.; *Aircraft operations from runways with inclined ramps (ski-jump)*. Wright Laboratory. Wright-Patterson AFB, Ohio, 1991
- [9] NASA TM 103866. Birckelbaw, L. *Ski Jump Takeoff Performance Predictions for a Mixed-Flow, Remote-Lift STOVL Aircraft*, 1992.
- [10] HM Government; *Securing Britain in an age of uncertainty: The Strategic Defence and Security Review*. Oct, 2010
- [11] <http://www.royalnavy.mod.uk/News-and-Events/Latest-News/2012/May/10/120509-F35B>
- [12] Fozard, John W. *The British Aerospace Harrier. Case study in aircraft design*. AIAA Professional Study Series, 1978.
- [13] Anderson, J.D., *Aircraft performance and design*. McGraw-Hill, Singapore, 1999.
- [14] Hull, D.G., *Fundamentals of airplane flight mechanics*. Springer Verlag, Berlin, 2007.
- [15] MIL-HDBK-2066(AS). *Catapulting and arresting gear forcing functions for aircraft structural design*. 1989.
- [16] www.shipbucket.com; JCI ship drawing, courtesy of MConrads, harpoon & Diego Alariste. Admiral Kuznetsov ship drawing, courtesy of Gollevainen
- [17] *Jane's all the world's aircraft*. Jane's information group.1990-2010.
- [18] NAWCADPAX/TR-2002/71. *Review of the carrier approach criteria for carrier-based aircraft. Phase I; final report*. 2002
- [19] SA FTM-01. *Carrier suitability testing manual*. NAWCAD, 1991
- [20] NAVAIR 00-80T-105. *CV NATOPS manual*. 2009
- [21] Cherry, B & Constantino, M. *The burble effect: superstructure and flight deck effects on carrier air wake*. US Naval Academy, 2010.
- [22] *LSO reference manual*. US Navy landing signals officer school. 1999
- [23] NAVAIR 00-80T-104. *NATOPS Landing signal officer manual*. 2001
- [24] www.fas.org/irp/doddir/navy/rfs/part02.htm and z11.invisionfree.com/shipbucket/ar/t2641.htm
- [25] AIAA 2004-5026. Young, Jennifer. *X-31 VECTOR Program Summary*. AIAA Guidance, Navigation and Control Conference and Exhibit, 2004. DTNSRDC-83/020, 2004.

Copyright Statement

The authors confirm that they, and/or their company or organization, hold copyright on all of the original material included in this paper. The authors also confirm that they have obtained permission, from the copyright holder of any third party material included in this paper, to publish it as part of their paper. The authors confirm that they give permission, or have obtained permission from the copyright holder of this paper, for the publication and distribution of this paper as part of the ICAS2012 proceedings or as individual off-prints from the proceedings.